Adsorption of Methane from Hydrogen on Fixed Beds of Silica Gel

M. LARRY CAMPBELL and LAWRENCE N. CANJAR

Carnegie Institute of Technology, Pittsburgh, Pennsylvania

An extensive research program has been undertaken to obtain data on a variety of adsorption systems exhibiting different characteristics in order to obtain a general model for representing adsorption data. This paper deals with the adsorption of methane from a hydrogen gas stream by various sizes of silica gel particles in fixed beds.

EXPERIMENTAL APPARATUS AND PROCEDURE

The experimental apparatus used to obtain break curves was the same as Geser's (*1*) and essentially consisted of an adsorption complex immersed in a constant temperature bath at roughly —115°F. The complex was fed by cylinders of pure hydrogen and prepared mixtures of methane in hydrogen. The gas flow rate was measured by incremental timing of a wet test meter. Figure 1 is a flow sheet for the process.

The adsorption complex consisted of three 1-in. diam. sections. The first section was 15 in. long and the next two were 6 in. long. The sections were connected by flanges which utilized beveled metal-to-metal seals. These flanges contained a concentration measuring thermistor and a pressure tap which was connected to a calibrated inclined mercury manometer. The bead thermistors were employed with a bridge circuit to form a thermal conductivity cell. A copper-constantan thermocouple was inserted in the first 6-in. bed. The electromotive forces from the thermistor bridge and the bed thermocouple were programed with motor-driven multicam switches and two-pole relays to a single-point self-balancing recording potentiometer.

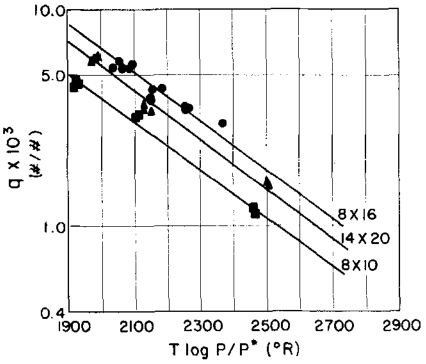

Fig. 2. Equilibrium data (polanyi method).

The beds were packed with a ½-in. layer of 2-mm. glass beads and then the prepared sample of adsorbent. They were purged with hydrogen at room temperature for about 2 hr. and then put in the cold bath until the equipment and thermistors reached thermal equilibrium.

A run was initiated by switching the feed gas from hydrogen to the desired gas mixture. When the effluent gas reached the feed concentration and held steady for 5 min., the run was switched to hydrogen. The desorption curve found in this manner was also recorded.

When the concentration returned to zero, the gas flow rate was adjusted, and the next run was started. Numerous runs were taken in this manner with no noticeable decrease in adsorptive capacity.

Data* were obtained on 8 × 10 and 8 × 16 mesh size particles of A silica gel and 14 × 20 mesh size of Grade 08. The samples were activated by heating them at 350°F. for approximately 24 hr.

THEORY AND DATA ANALYSIS

If one assumes constant plug flow, isothermal conditions, negligible radial concentration gradients, and negligible axial dispersion, the following material balance for a differential element of adsorption bed can be written:

$$F\left(\frac{\partial C}{\partial z}\right)_t + \epsilon A\left(\frac{\partial C}{\partial t}\right)_z + \frac{A\rho_B}{M}\left(\frac{\partial q}{\partial t}\right)_z = 0 \qquad (1)$$

From C vs. t curves for given points in the adsorption bed the second term of Equation (1) was calculated, and a cross plot of this same data into the form c vs. z for given t gave values for the first term. In this way the rate term $\left(\frac{\partial q}{\partial t}\right)_z$ was experimentally determined for various times and positions in the bed.

This rate of adsorption involves three principal mechanisms:

1. Transfer of the adsorbate from the flowing fluid to the external surface of the particle.
2. Diffusion into the particle.
3. Attachment of the adsorbate to an adsorption site.

Mechanism 3 is extremely rapid, and the concentration of the adsorbate in the gas phase at the gas-solid interface is assumed to be the equilibrium value corresponding to the amount adsorbed at the interface. It can be shown for this system that mechanism 1 is reasonably fast. By use of the mass transfer correlation of Hougen and Watson (5)

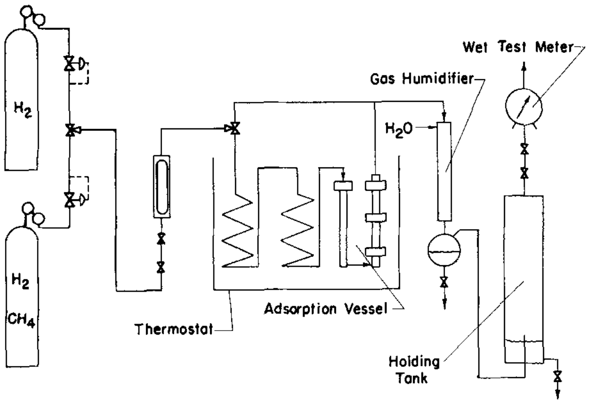

Fig. 1. Flow sheet.

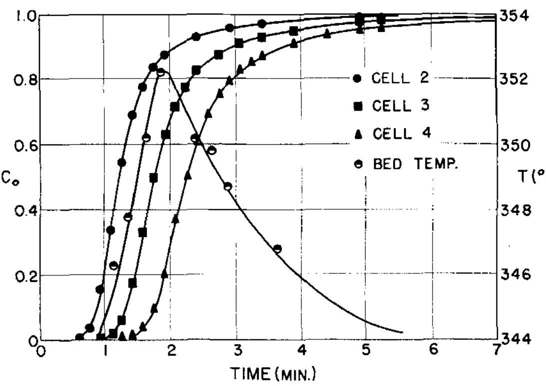

Fig. 3. Concentration profiles.

M. Larry Campbell is with the Esso Research and Engineering Company, Linden, New Jersey.

* Detailed data are available in a doctoral thesis by M. L. Campbell, Carnegie Institute of Technology, Pittsburgh, Pennsylvania.

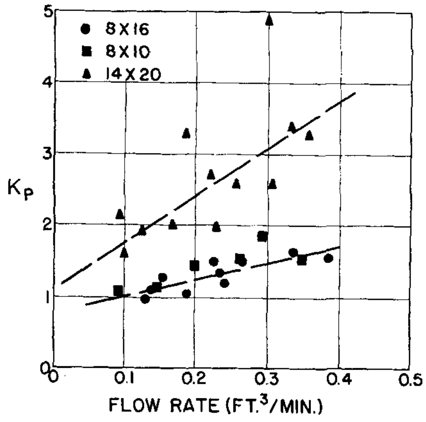

Fig. 4. Effect of flow rate on particle transfer coefficients.

the difference in concentration of the adsorbate in the bulk fluid and the concentration at the interface is estimated to be less than 0.007 mole fraction for all particle sizes. This is insignificant compared with the accuracy of the data.

The rate of adsorption can therefore be described in terms of mechanism 2. The rate expressions developed by Hiester and Vermeulen (*3*, *4*), Thomas (*7*, *8*), and Glueckauf (*2*) were investigated as possible representations of the data obtained in the work. These solutions and methematical models failed, and it was necessary to develop a new mathematical model.

It is postulated that the rate of transfer of material from the particle surface inward is proportional to the difference between the ultimate capacity of the particle for the adsorbate and the concentration of the adsorbate on the particle surface:

$$\frac{dq}{dt} = K_p\,(Q_\infty - q^*) \qquad (2)$$

It is further postulated that the ultimate or equilibrium capacity of the bed is not constant but is related to the amount of hydrogen retained on the bed by the following expression:

$$Q_\infty = (1 - x_{H_2})\,q_\infty \qquad (3)$$

where

$$x_{H_2} = \left(\frac{q}{q_\infty}\right)_{H_2} \qquad (4)$$

Equation (2) becomes

$$\frac{dq}{dt} = K_p\,[(1 - x_{H_2})\,q_\infty - q^*] \quad (5)$$

where K_p is dependent on gas flow rate, such a dependence does not indicate a fluid diffusional resistance. It should be noted that Equation (5) holds at the limiting conditions. Before breakthrough $x_{H_2} = 1$, $q^* = 0$, and $dq/dt = 0$. At saturation of the bed $x_{H_2} = 0$, $q^* = q_\infty$, and $dq/dt = 0$.

Calculational Procedure

1. The amount of methane adsorbed at saturation was calculated by graphically integrating the area above the effluent curve. These values were then plotted against the Polanyi adsorption potential, $RT \ln P/p^*$, which represents the free energy of compression of 1 mole of gas from the equilibrium adsorption pressure to the vapor pressure P. The equilibrium data are plotted in this manner for each particle size on Figure 2.

2. Equation (1) was used to find $(\partial q/\partial t)_z$ at various points on the break curve. These values were obtained at the middle cell, since this is the point of maximum precision.

3. The temperature data were plotted and smoothed, and values of T were obtained at each of the points where $(\partial q/\partial t)_z$ was calculated in step 2. The breakthrough curves and associated temperature profile for a typical run are shown on Figure 3.

4. From the cell pressure, bed temperature, C^*, and the vapor pressure of methane at the bed temperature the adsorption potential was calculated, and q^* was taken from Figure 2.

TABLE 1. PARTICLE TRANSFER COEFFICIENTS

Run no.	Inlet gas concentration, (mole) (% CH_4)	F, (std. cu. ft./min.)	K_p, (1/min.)
8 × 16 silica gel			
2	10.65	0.191	1.052
3	10.65	0.269	1.492
4	10.65	0.345	1.635
5	10.65	0.156	1.262
6	7.58	0.138	1.085
7	7.58	0.239	1.328
9	7.58	0.398	1.542
10	5.69	0.128	0.953
11	5.69	0.243	1.175
17	7.58	0.222	1.488
8 × 10 silica gel			
42	7.58	0.254	2.03
43	7.58	0.088	1.07
47	2.54	0.140	1.16
48	2.54	0.344	1.52
49	2.54	0.196	1.44
54	12.44	0.302	1.85
14 × 20 silica gel			
57	12.44	0.121	1.90
58	12.44	0.167	1.97
59	12.44	0.221	2.70
60	12.44	0.302	4.86
61	7.58	0.093	2.12
62	7.58	0.186	3.62
63	7.58	0.256	2.56
64	7.58	0.344	3.38
65	2.54	0.100	1.58
66	2.54	0.230	1.93
67	2.54	0.309	2.56
68	2.54	0.369	3.26

Atmospheric pressure, bath temperature = 115°F.

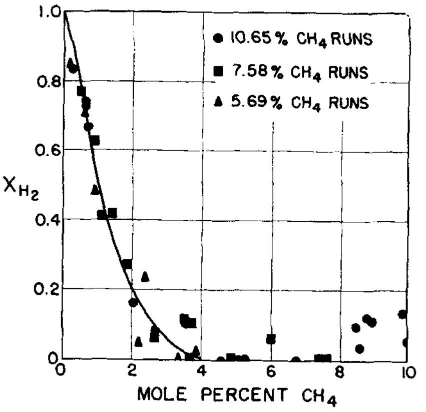

Fig. 5. Relationship between hydrogen on bed and gas concentration, 8 × 16 silica gel.

5. With values found in the previous steps a particle transfer coefficient K_p was assumed and x_{H_2}'s were calculated for a run with Equation (5). K_p was adjusted until x_{H_2} was never negative. The results of these calculations are in the next section.

RESULTS

Particle Transfer Coefficient

The value of K_p for each run is given in Table 1. The K_p's are not constant for each run but show a trend with flow rate. K_p is plotted vs. flow rate on Figure 4. This trend is more pronounced with the smaller particle size.

Although particle transfer coefficients are expected to be constant and not a function of flow rate, other investigators (*6*) have noticed this trend in their particle coefficient.

A number of reasons can be given for this trend. The most important is that experimental temperature profile may be lower than the actual case around the peak of the profile. This deviation would be greatest at the highest flow rates. If this were so, q^* would be smaller, and looking at Equation (5) one can see that this would reduce K_p. Also a fluid flowing past a pore may affect diffusion in the pore to a small extent. Another reason may be that the mass transfer correlations are incorrect. If this is true, the flow rate effect on the external mass transfer would have to be put in the particle coefficient. Finally the effective transfer area may change with flow rate, which may affect the value of the particle transfer coefficient.

There appears to be no dependency of K_p upon inlet gas concentration or bed length. K_p's were found at other lengths and checked quite closely considering the errors produced in taking slopes.

x_{H_2}'s

The quantity x_{H_2} is plotted against gas concentration on Figure 5 for all runs taken on the 8 × 16 particle size. It can be seen that x_{H_2} becomes zero around a gas concentration of 4 mole % methane. In other words when concentration of 4 mole % methane is reached on the breakthrough curve, no hydrogen remains adsorbed on the bed. For the other particle sizes x_{H_2} becomes zero at roughly the same concentration.

After the zero was dropped, x_{H_2} did not remain constant but became slightly positive for some of the runs. This deviation was most serious for the high flow rate runs because the slopes of the curves used to find $(\partial q/\partial t)_z$ were steepest in these cases and therefore less precise.

Another reason for this deviation may be that the experimentally measured temperature lagged behind the true bed temperature toward the end of a run. If one considers Equation (5), it can be seen that if the true temperature is lower than that measured q^* will be higher, and in turn x_{H_2} will be lower.

SUMMARY

A rate equation is presented which describes data obtained on the adsorption of methane from hydrogen by silica gel. The bed temperature has been used and the adsorption rates have been calculated without making the usual simplifying assumption. The particle transfer coefficient is dependent on flow rate, and the quantity x_{H_2} seems to have a definite relationship with gas concentration.

The model has been applied to a system with a linear equilibrium adsorption isotherm in this paper and in a previous work (*1*) to a system with a favorable equilibrium or constant pattern. In view of these facts the utility of this model is felt to be demonstrated.

ACKNOWLEDGMENT

This research was supported by a grant from the Petroleum Research Fund administered by the American Chemical Society. Grateful acknowledgment is hereby made to the donors of this fund.

NOTATION

A = cross-sectional area of bed, sq. ft.
C = concentration of adsorbate in fluid phase, mole/cu. ft.
C^* = interface gas concentration, mole/cu. ft.
F = volumetric flow rate, cu. ft./min.
K_p = particle transfer coefficient, 1/min.
M = molecular weight
p = partial pressure of methane in gas stream, atm.
p^* = interface partial pressure of methane, atm.
q = average adsorbate concentration in particle, lb. adsorbate/lb. adsorbent
q^* = adsorbate concentration of particle at interface, lb. adsorbate/lb. adsorbent
q_∞ = adsorbate concentration in equilibrium with C_∞, lb adsorbate/lb. adsorbent
Q_∞ = $(1 - x_{H_2})\, q_\infty$
t = time, min.
T = temperature
x_{H_2} = $(q/q_\infty)_{H_2}$
z = bed length
ϵ = bed porosity, cu. ft. void/cu. ft. bed
ρ_B = bulk density, lb. adsorbent/cu. ft. bed

LITERATURE CITED

1. Geser, J. J., Ph.D. dissertation, Carnegie Inst. Technol., Pittsburgh, Pennsylvania (1961).
2. Glueckauf, E., *Trans. Faraday Soc.*, **51**, 1540 (1955).
3. Hiester, N. K., et al., *A.I.Ch.E. Journal*, 2, 404 (1956).
4. Hiester, N. K., and Theodore Vermeulen, *Chem. Eng. Progr.*, **48**, 505 (1952).
5. Hougen, O. A., and K. W. Watson, "Chemical Process Principles," Part 3, p. 987, Wiley, New York (1947).
6. Moison, R. L., and H. A. O'Hearn, Jr., *Chem. Eng. Progr. Symposium Ser. No. 24*, **55**, 71 (1959).
7. Thomas, H. C., *J. Am. Chem. Soc.*, **66**, 1664 (1944).
8. ———, *Ann. N. Y. Acad. Sci.*, **49**, 161 (1948).

Manuscript received October 13, 1961; revision received February 5, 1962; paper accepted February 6, 1962. Paper presented at A.I.Ch.E. Los Angeles meeting.

Heat Transfer from a Cylinder to a Power-Law Non-Newtonian Fluid

M. J. SHAH, E. E. PETERSEN, and ANDREAS ACRIVOS
University of California, Berkeley, California

For low-molecular-weight liquids and for all gases it has been postulated and repeatedly verified experimentally that the shear stress imposed on the fluid is directly proportional to the rate of strain at constant temperature and pressure. The proportionality constant in this linear relation is called the *viscosity* and for the simple one-dimensional flow is defined by

$$\mu = \frac{\tau}{du/dy} \tag{1}$$

It is found however that for many fluids—solutions of organic macromolecules, pulps, slurries, molten plastics, etc.—the viscosity coefficient in Equation (1), instead of being only a property of the material and thus independent of its state of motion, is also markedly affected by changes in the shear rate. It is clear therefore that for such rheological substances, which are grouped together under the common name *non-Newtonian fluids*, the concept of viscosity is a rather useless one and that an expression different from Equation (1) must be sought to relate the local stress to the hydrodynamic variables of the system.

In the past various models relating shear rate and shear stress have been proposed for different types of non-Newtonian behavior (*7*). Among the more commonly encountered expressions are those for Bingham plastic fluids, for which

$$\tau - \tau_y = \eta \left(\frac{du}{dy}\right) \tag{2}$$

and those for power-law fluids, where, again for one-dimensional flow conditions

$$\tau = K \left(\frac{du}{dy}\right)^n \tag{3}$$

with $n < 1.0$ for pseudoplastics and $n > 1.0$ for dilatant substances.

The functional relation between the stress and the state of motion of the fluid, the so-called *rheological equation of state*, must as a rule be obtained experimentally. Even so, the interpretation of the experimental results is seldom unequivocal because in general the stress is a function not only of the rate of strain, but also of the higher

---

M. J. Shah is with International Business Machines Corporation, San Jose, California. Andreas Acrivos is at Stanford University, Stanford, California.